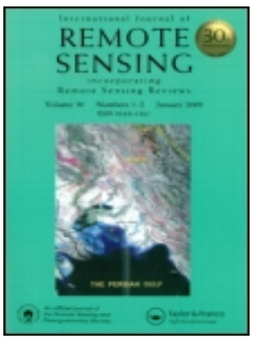

International Journal of Remote Sensing

ISSN: 0143-1161 (Print) 1366-5901 (Online) Journal homepage: http://www.tandfonline.com/loi/tres20

Evaluation of four MERIS atmospheric correction algorithms in Lake Kasumigaura, Japan

Lalu Muhamad Jaelani, Bunkei Matsushita, Wei Yang & Takehiko Fukushima

To cite this article: Lalu Muhamad Jaelani, Bunkei Matsushita, Wei Yang & Takehiko Fukushima (2013) Evaluation of four MERIS atmospheric correction algorithms in Lake Kasumigaura, Japan, International Journal of Remote Sensing, 34:24, 8967-8985, DOI: 10.1080/01431161.2013.860660

To link to this article: http://dx.doi.org/10.1080/01431161.2013.860660

Published online: 18 Nov 2013.

International Journal of Remote Sensing, 2013
Vol. 34, No. 24, 8967–8985, http://dx.doi.org/10.1080/01431161.2013.860660

Taylor & Francis
Taylor & Francis Group

Evaluation of four MERIS atmospheric correction algorithms in Lake Kasumigaura, Japan

Lalu Muhamad Jaelani[a], Bunkei Matsushita[a]*, Wei Yang[a,b], and Takehiko Fukushima[a]

[a]*Graduate School of Life and Environmental Sciences, University of Tsukuba, Tsukuba, Ibaraki 305-8572, Japan;* [b]*State Key Laboratory of Earth Surface Processes and Resource Ecology, Beijing Normal University, Beijing 100875, China*

(*Received 14 January 2013; accepted 30 September 2013*)

Accurate atmospheric correction for turbid inland waters remains a significant challenge. Several atmospheric correction algorithms have been proposed to address this issue, but their performance is unclear in regard to Asian lakes, some of which have extremely high turbidity and different inherent optical properties from lakes in other continents. Here, four existing atmospheric correction algorithms were tested in Lake Kasumigaura, Japan (an extremely turbid inland lake), using *in situ* water-leaving reflectance and concurrently acquired medium resolution imaging spectrometer (MERIS) images. The four algorithms are (1) GWI (the standard Gordon and Wang algorithm with an iterative process and a bio-optical model) (2) MUMM (Management Unit of the North Sea Mathematical Models); (3) SCAPE-M (Self-Contained Atmospheric Parameters Estimation for MERIS Data) and (4) C2WP (Case-2 Water Processor). The results show that all four atmospheric correction algorithms have limitations in Lake Kasumigaura, even though SCAPE-M and MUMM gave acceptable accuracy for atmospheric correction in several cases (relative errors less than 30% for the 2006 and 2008 images). The poor performance occurred because the conditions in Lake Kasumigaura (i.e. the atmospheric state and/or turbidity) did not always meet the assumptions in each atmospheric correction algorithm (e.g. in 2010, the relative errors ranged from 42% to 83%). These results indicate that further improvements are necessary to address the issue of atmospheric correction for turbid inland waters such as Lake Kasumigaura, Japan.

1. Introduction

Lakes play important roles as freshwater resources for drinking water, agriculture, industry, fishing, recreation, and tourism (Giardino et al. 2001). However, accelerated eutrophication in lakes is becoming a significant environmental issue around the world (Ayres et al. 1996). Water quality monitoring is thus a critical requirement for water resource management in order to support the sustainable development of freshwater ecosystems. In light of the spatial and temporal heterogeneities of water bodies, remote sensing techniques can be an effective approach for the routine monitoring of water quality (Liu, Islam, and Gao 2003).

The first key step for water colour remote sensing is atmospheric correction. A widely used atmospheric correction algorithm with sufficient accuracy was developed by Gordon and Wang (1994) for clear waters (e.g. open oceans). However, this algorithm has often been reported to fail in coastal and inland waters because its assumption of negligible water-leaving reflectance at near-infrared (NIR) wavelengths becomes invalid in these

*Corresponding author. Email: matsushita.bunkei.gn@u.tsukuba.ac.jp

turbid waters (Hu, Carder, and Muller-karger 2000; Shi and Wang 2007, 2009; Wang, Son, and Shi 2009). Several efforts have been made to solve this problem. Currently, there are five types of approach for atmospheric correction over turbid waters (inland or coastal waters, Table 1).

The first type of approach is based on the estimation of water-leaving reflectance (or radiance) at two NIR reference wavelengths rather than neglecting the water-leaving reflectance (or radiance) at these two wavelengths (Hu, Carder, and Muller-karger 2000; Stumpf et al. 2003; Bailey, Franz, and Werdell 2010; Wang, Shi, and Jiang 2012). For example, Stumpf et al. (2003) and Bailey, Franz, and Werdell (2010) suggested the use of a bio-optical model to estimate water-leaving reflectance at two NIR reference wavelengths through an iterative procedure. This approach is now widely used for atmospheric correction over turbid waters.

The second type of approach is based on the direct prediction of atmospheric parameters over water pixels (Ruddick, Ovidio, and Rijkeboer 2000; Guanter et al. 2010). For example, Ruddick, Ovidio, and Rijkeboer (2000) proposed the use of two new assumptions rather than the assumption in Gordon and Wang (1994) to estimate multiple-scattering aerosols and aerosol-Rayleigh reflectances at two reference NIR wavelengths. Guanter, Sanpedro, and Moreno (2007) and Guanter et al. (2010) proposed the use of atmospheric parameters derived over neighbouring land pixels to predict atmospheric parameters over close-to-land water pixels through a spatial extension method; this can avoid assumptions on water composition and its spectral response.

The third type of approach is based on neural network (NN) techniques (Doerffer and Schiller 2007, 2008; Schroeder, Schaale, and Fischer 2007; Schroeder et al. 2007).

Table 1. Summary of existing atmospheric correction algorithms for turbid waters.

Type	Approach descriptions	References for example
1	Estimation of water-leaving reflectance at two NIR reference wavelengths; subtraction of the estimated water-leaving reflectance from TOA remote-sensing reflectance at two NIR reference wavelengths; application to Gordon and Wang's (1994) scheme for atmospheric correction.	Hu, Carder, and Muller-karger (2000); Stumpf et al. (2003); Bailey, Franz, and Werdell (2010) and Wang, Shi, and Jiang (2012)
2	Direct prediction of atmospheric parameters over water pixels; application to Gordon and Wang's (1994) scheme or other methods for atmospheric correction.	Ruddick, Ovidio, and Rijkeboer (2000); Guanter et al. (2010)
3	Neural network (NN) techniques	Schroeder, Schaale, and Fischer (2007); Schroeder et al. (2007); Doerffer and Schiller (2007, 2008)
4	Keep the assumption of zero water-leaving reflectance but extend the reference wavelengths from NIR to SWIR for turbid water pixels; application to Gordon and Wang's (1994) scheme for atmospheric correction.	Wang and Shi (2007)
5	Spectral optimization techniques	Kuchinke et al. (2009); Kuchinke, Gordon, and Franz (2009)

Note: NIR: near infrared; TOA: top-of-atmosphere; SWIR: shortwave infrared.

For example, Doerffer and Schiller (2008) designed an algorithm to directly estimate remote-sensing reflectance at the bottom-of-atmosphere (BOA) from that at the top-of-atmosphere (TOA) based on separate NNs. The fourth type of approach still keeps the assumption of zero water-leaving reflectance but extends the reference wavelengths from NIR to shortwave infrared (SWIR) for turbid water pixels (Wang and Shi 2007). The fifth type of approach is based on spectral optimization (Kuchinke et al. 2009; Kuchinke, Gordon, and Franz 2009). In this approach, absorbing aerosol models and a bio-optical reflectance model were combined to provide the TOA reflectance; the modelled TOA reflectance was then fitted to the observed TOA reflectance through non-linear optimization to determine the parameters of both models. These parameters were then gradually improved through an iterative procedure to accomplish atmospheric correction.

Medium resolution imaging spectrometer (MERIS) has 15 narrow spectral bands in the visible and NIR spectral ranges (most bandwidths are around 10 nm) and a medium spatial scale (about 300 m for full spatial resolution data). Regarding spectral configuration and spatial resolution, MERIS offers the best compromise between spatial, spectral, and temporal resolution for many inland water studies (although since April 2012 MERIS has no longer been providing data, the next-generation sensors will be launched in 2014; Aschbacher and Perez [2012]). In addition, the availability of an atmospheric correction algorithm for public use is also expected.

Therefore, we used two criteria for selecting the algorithms: (1) applicability to MERIS data; and (2) current or expected future implementation into the widely used processing software packages SeaDAS (SeaWiFS Data Analysis System; http://seadas.gsfc.nasa.gov) and BEAM (Basic ERS & ENVISAT AATSR and MERIS; http://www.brockmann-consult.de/cms/web/beam). Based on these two criteria, we selected four existing atmospheric correction algorithms for an evaluation of their performance in this study. We selected one atmospheric correction algorithm from the first type of approach and another from the second type. Both are currently available in SeaDAS software for processing level-1b data from satellite sensors such as SeaWiFS (Sea-viewing Wide Field-of-view Sensor), MODIS (Moderate Resolution Imaging Spectroradiometer), and MERIS.

Another atmospheric correction algorithm was chosen from the third type of approach, which is currently available in the BEAM toolbox. We selected the fourth atmospheric correction algorithm from the second type of approach, which will be available in the BEAM toolbox in the near future. Although the fourth and fifth types of approach are available in SeaDAS software, they can only be applied to MODIS and SeaWiFS data (not available for MERIS), respectively, and thus they were not used in this study. More details about the four selected atmospheric correction algorithms can be found in Section 2.1.

Although several of the above-mentioned algorithms have been evaluated using a simulated testing dataset (e.g. IOCCG 2010) or *in situ* measurements from coastal waters (e.g. Jamet et al. 2011) or European lakes (e.g. Guanter et al. 2010), few studies have been designed to evaluate for turbid Asian lakes to show the applicability of these algorithms (Wang, Shi, and Tang 2011; Duan et al. 2012). The objectives of the present study were thus: (1) to evaluate the four selected atmospheric correction algorithms by comparing the atmospherically corrected remote-sensing reflectance from three MERIS images using the algorithms with concurrent *in situ* remote-sensing reflectance obtained from three data collection campaigns in Lake Kasumigaura, Japan; and (2) to investigate the validity of the assumptions in the four atmospheric correction algorithms to understand the advantages as well as the limitations of each algorithm.

2. Methods

2.1. Four atmospheric correction algorithms

The first selected atmospheric algorithm was developed by Stumpf et al. (2003) and updated by Bailey, Franz, and Werdell (2010). This algorithm is based on the original atmospheric correction scheme proposed by Gordon and Wang (1994), denoted as GW94 hereafter, which is based on the assumption of negligible water-leaving radiance at an NIR band, but the algorithm can avoid the over-correction of the atmospheric signal for waters where the assumption in the GW94 is not valid (Bailey, Franz, and Werdell 2010).

In the algorithm, water-leaving reflectance at two NIR reference bands was first estimated by a bio-optical model. Then the two estimated water-leaving reflectance values were removed from corresponding remote-sensing reflectance at the TOA, and inputted into the GW94 algorithm. The iterative procedure makes the estimated water-leaving reflectance by the bio-optical model gradually close to the actual water-leaving reflectance (the algorithm allows up to 10 iterations, but it will converge after 3–4 in most cases; Bailey, Franz, and Werdell 2010). Therefore, this algorithm is hereafter called the GWI algorithm (standard Gordon and Wang's algorithm with an iterative process and a bio-optical model). The new assumption in the GWI algorithm is that the bio-optical model used can provide accurate estimates of water-leaving reflectance at two NIR reference wavelengths.

The second selected atmospheric correction algorithm is MUMM (Management Unit of the North Sea Mathematical Models), which was proposed by Ruddick, Ovidio, and Rijkeboer (2000). This algorithm is also based on the original atmospheric correction scheme in GW94. The MUMM algorithm uses two different assumptions as a replacement for the original assumption in GW94 (i.e. zero water-leaving reflectance at NIR bands), according to the stable spectral shapes of aerosol and water-leaving reflectances at two NIR reference bands.

Ruddick et al. (2006) assumed that the ratios of (1) multiple-scattering aerosols and aerosol-Rayleigh reflectances and (2) water-leaving reflectance normalized by the sun–sea atmospheric transmittance at two NIR reference bands are spatially homogeneous over the sub-scene of interest (the former was named ε and the latter, α; Ruddick, Ovidio, and Rijkeboer 2000). These two new assumptions allow the estimates of multiple-scattering aerosols and aerosol-Rayleigh reflectances at two NIR reference bands even for waters where water-leaving reflectance cannot be ignored. The estimated multiple-scattering aerosols and aerosol-Rayleigh reflectance at two NIR reference bands are then inputted into the original GW94 algorithm for atmospheric correction in turbid waters. Thus, the performance of the MUMM algorithm depends not only on water composition and its spectral response (this is the definition of α), but also on the atmosphere status over the target waters (the definition of ε).

The third atmospheric correction algorithm selected for comparison is the SCAPE-M (Self-Contained Atmospheric Parameters Estimation for MERIS Data) algorithm (Guanter, Sanpedro, and Moreno 2007; Guanter et al. 2010). Unlike the traditional atmospheric correction algorithms for waters, which are 'water-based' methods, the SCAPE-M is a 'land-based' method for the retrieval of aerosol and water-leaving reflectances. Therefore, the SCAPE-M algorithm requires neither *a priori* assumptions about water composition and its spectral response nor the use of bio-optical models. It uses atmospheric parameters derived over neighbouring land pixels to predict atmospheric parameters over close-to-land water pixels through a spatial extension method.

In the SCAPE-M algorithm, aerosol retrieval is performed at the macro-pixel scale. First, a MERIS Level-1b image is divided into a series of macro-pixels (30 km × 30 km). For each macro-pixel, a maximum AOT550 (aerosol optical thickness at 550 nm) is estimated from dark pixels in the area to avoid negative reflectance after atmospheric correction. This value is then refined by the exploitation of those macro-pixels with sufficient green vegetation and bare soil pixels (generally, five land pixels that show mixed vegetation and bare soil with as much spectral contrast as possible are needed). By assuming that surface reflectance can be provided by a linear combination of two endmembers (i.e. pure vegetation and bare soil), the abundance of each endmember and the AOT550 are retrieved concurrently for each macro-pixel.

Finally, the obtained AOT550 is applied to water pixels for atmospheric correction by assuming that the atmospheric state is laterally homogeneous within each macro-pixel. Because of the above assumptions, the SCAPE-M algorithm can only be used for small- and medium-sized water bodies. In addition, only a rural aerosol model is used in the SCAPE-M algorithm because less information is available for the reliable retrieval of aerosol type over land from MERIS (Santer, Vidot, and Aznay 2005; Ramon and Santer 2005). The SCAPE-M algorithm will be available in the BEAM toolbox in the near future (L. Guanter, personal communication).

The last selected atmospheric correction algorithm is the Case-2 Water Processor (C2WP), which is available in the BEAM toolbox (Doerffer and Schiller 2008). The C2WP algorithm contains three different processors: the *Case-2 Regional* water processor, the *Eutrophic Lakes* processor, and the *Boreal Lakes* processor. The three processors share the same architecture, but the bio-optical models were optimized for different concentrations of chlorophyll-*a*, total suspended mater (TSM), and yellow substance. The NNs for atmospheric correction were trained based on the radiative transfer (RT)-simulated water-leaving reflectance at both the BOA and the TOA by taking into account various atmospheric and oceanic conditions.

To generate water-leaving reflectance from RT simulations at the BOA, the inherent optical properties (IOPs) were taken from European coastal waters, Spanish lakes, and Finnish lakes. By considering the water quality parameters in Lake Kasumigaura, Japan, the *Eutrophic Lakes* processor (version 1.5.7) was selected for atmospheric correction in the present study. The concentration ranges covered in the simulations for the *Eutrophic Lakes* processor were 1–120 mg m^{-3} for chlorophyll-*a*, 0.433–51.9 g m^{-3} for TSM, and 0.1–3.0 m^{-1} (at 443 nm) for yellow substance. The C2WP algorithm was designed for European waters, and it is worthwhile to evaluate the performance of this algorithm in Asian waters.

2.2. Data

To evaluate the above-mentioned atmospheric correction algorithms in turbid inland waters, we collected concurrent *in situ* and MERIS data from Lake Kasumigaura, Japan. The lake is located in the eastern part of Japan's Kanto plain and has a surface area of 171 km^2 (western part only), an average depth of 4.0 m, and a maximum depth of 7.3 m. It is the second largest lake in Japan (Lake Biwa is the largest) and it is a eutrophic-turbid lake due to high loading of nutrients and resuspension of bottom sediments by wind (Fukushima et al. 1996; Oyama et al. 2009). During the previous two or three decades, Lake Kasumigaura's average TSM concentration has increased from 14.1 to 26.4 g m^{-3} (mainly due to the resuspension of bottom sediments by wind); chlorophyll-*a*

Table 2. Orbital information for three MERIS images used in this study (UTC: Coordinated Universal Time).

MERIS Data	K06	K08	K10
Orbit	20755	33652	42942
Acquisition date	18 February 2006	7 August 2008	18 May 2010
Starting time (UTC)	1:13:47	0:56:48	0:59:28
Ending time (UTC)	1:15:26	0:58:26	1:01:06
Sun Zenith (°)	53.04696	31.16381	27.08951
Sun Azimuth (°)	149.56363	122.01693	121.66913
View Zenith (°)	19.64261	14.39096	10.24573
View Azimuth (°)	285.36258	102.55517	102.91293

concentration decreased from 87 to 61 mg m^{-3} (owing to watershed management by the local government); and Secchi disk depth has decreased from 70 to 52 cm (CGER 2010).

Three full-resolution MERIS images (level-1b) covering Lake Kasumigaura were acquired on 18 February 2006 (denoted as K06 hereafter), 7 August 2008 (denoted as K08 hereafter), and 18 May 2010 (denoted as K10 hereafter). The orbital information for the three MERIS images is summarized in Table 2. These satellite images were processed using the SeaDAS (version 6.4) and BEAM (version 4.10.03) software packages to obtain atmospherically corrected water-leaving reflectance images by the GWI, MUMM, and C2WP algorithms. Since the SCAPE-M is not yet available for public use, we asked the algorithm's author (Dr Luis Guanter) to process the MERIS data using the SCAPE-M algorithm.

Three data collection campaigns were undertaken in 2006 (February 18, 10 sites), 2008 (August 7, 14 sites), and 2010 (May 18, 26 sites) in Lake Kasumigaura, and the campaigns were timed to coincide with acquisition of MERIS images. The spatial distribution of the sampling sites is shown in Figure 1. All reflectance measurements and water sample collections were performed between 10:00 and 14:00 h local time over optically deep waters. The water-leaving radiance ($L_u(\lambda)$), downward irradiance ($E_d(\lambda)$),

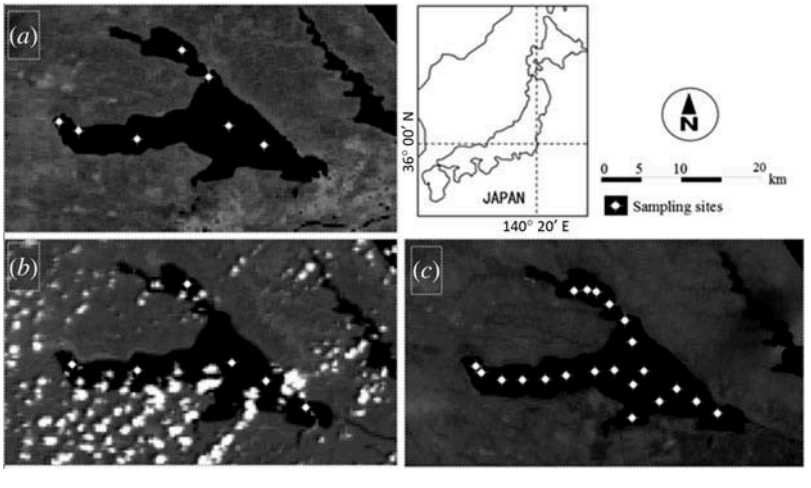

Figure 1. MERIS images and sampling sites at Lake Kasumigaura, Japan on (*a*) 18 February 2006, (*b*) 7 August 2008, and (*c*) 18 May 2010.

and downward radiance of skylight ($L_{sky}(\lambda)$) were measured at each site using a FieldSpec HandHeld (or Pro VNIR) spectroradiometer (Analytical Spectral Devices, Boulder, CO, USA) in the range of 325–1075 nm at 1 nm intervals. The above-water remote-sensing reflectance ($R_{rs}(\lambda)$) was approximated using the following equation (Mobley 1999):

$$R_{rs}(\lambda) = \left(\frac{L_u(\lambda)}{E_d(\lambda)} - \frac{rL_{sky}(\lambda)}{E_d(\lambda)}\right) \times \text{Cal}\ (\lambda), \quad (1)$$

where Cal(λ) is the spectral reflectance of the grey reference panel, which has been accurately calibrated, and r represents a weighted surface reflectance for the correction of surface-reflected skylight and is determined as a function of wind speed (Mobley 1999).

Water samples were kept in ice boxes and taken to the laboratory within approximately 0.5 h of whole-data collections. Chlorophyll-*a* was extracted using methanol (100%) at 4°C under dark conditions for 24 h. The optical density of the extracted chlorophyll-*a* was measured at four wavelengths (750, 663, 645, and 630 nm), and the concentration was calculated according to SCOR–UNESCO equations (SCOR-UNESCO 1966). Total suspended solids (TSS) were determined gravimetrically. Samples were filtered through a filter pre-combusted at 500°C for 4 h to remove dissolved organic matter in suspension, and the filter was then dried at 105°C for 4 h and weighed to obtain the TSS. The absorption of coloured dissolved organic matter (CDOM) was measured using a spectrophotometer (UV–1700, Shimadzu, Kyoto, Japan) with filtered water. Descriptive statistics of the optical water quality parameters are summarized in Table 3, in which it can be seen that the turbidity of Lake Kasumigaura is very high.

To evaluate the performance of the four atmospheric correction algorithms, we extracted the average water-leaving reflectance of the pixels nearest the sampling locations along with the eight surrounding pixels (3 × 3 window) from the atmospherically corrected MERIS images, and we compared reflectance with the corresponding *in situ* measurements. The use of the 3 × 3 window rather than a single pixel can reduce the

Table 3. Descriptive statistics of optical water quality parameters measured in Lake Kasumigaura, Japan.

	Min.	Max.	Median	Average	SD	CV (%)	*N*
18 February 2006							
Chl-a (mg m^{-3})	69.65	95.02	84.54	83.99	9.69	11.54	7
TSS (g m^{-3})	22.00	46.10	32.80	33.71	8.11	24.05	7
$^{a}_{CDOM}$ (440) (m^{-1})	no data	no data	no data	no data	no data	no data	0
7 August 2008							
Chl-a (mg m^{-3})	44.40	76.90	62.90	62.18	11.92	19.17	6
TSS (g m^{-3})	11.70	21.10	16.40	16.73	3.18	19.02	6
$^{a}_{CDOM}$ (440) (m^{-1})	1.15	1.36	1.15	1.20	0.09	7.23	6
18 May 2010							
Chl-a (mg m^{-3})	36.60	83.40	44.80	53.70	17.61	32.80	21
TSS (g m^{-3})	18.00	27.73	21.17	22.13	3.59	16.22	21
$^{a}_{CDOM}$ (440) (m^{-1})	0.51	0.94	0.62	0.71	0.16	22.23	21

Notes: Chl-a, chlorophyll-a concentration; TSS, total suspended solids;
$^{a}_{CDOM}$ (440), absorption coefficient of CDOM at 440 nm;
SD, standard deviation; CV, coefficient of variation (= SD/average of parameter);
N, number of samples.

potential error in the geometric correction and dynamics of water bodies, as well as potential error in spatial variability (Han and Jordan 2005). Pixels contaminated by clouds and corresponding sampling sites located less than one pixel away from the banks were then excluded. Accordingly, 7, 6, and 21 sites remained for comparison in February 2006, August 2008, and May 2010, respectively.

2.3. Accuracy assessment

Two indices, root mean square error (RMSE) and relative error (RE), were used to assess the accuracy of atmospheric correction. These indices were defined as follows:

$$\mathrm{RMSE} = \sqrt{\frac{\sum_{i=1}^{N}\left(x_{\mathrm{esti},i} - x_{\mathrm{meas},i}\right)^2}{N}}, \tag{2}$$

$$\mathrm{RE} = \frac{1}{N}\sum_{i=1}^{N}\left(\sqrt{\left(\frac{x_{\mathrm{esti},i} - x_{\mathrm{meas},i}}{x_{\mathrm{meas}}}\right)^2}\right)100\%, \tag{3}$$

where $x_{\mathrm{meas},i}$ and $x_{\mathrm{esti},i}$ are the measured and estimated values, respectively, and N is the number of samples. RMSE gives the absolute scattering of the retrieved water-leaving reflectance while RE represents the uncertainty associated with satellite-derived distribution. The determination coefficient (R^2) between the *in situ*-measured $R_{\mathrm{rs}}(\lambda)$ and estimated $R_{\mathrm{rs}}(\lambda)$ from the atmospherically corrected MERIS data was also calculated.

3. Results

3.1. Performance of the four atmospheric correction algorithms for MERIS single bands

Figure 2 provides the overall comparisons between the measured (x-axis) and retrieved (y-axis) water-leaving remote-sensing reflectance values obtained by the four atmospheric correction algorithms at MERIS bands 1–10 for the three dates. Generally, the SCAPE-M algorithm overestimated the values of water-leaving reflectance at all MERIS bands (except for several bands in 2006), whereas the other three algorithms gave underestimation of water-leaving reflectance (except for bands 1, 2, and 10 for MUMM in 2008).

From the data collected in 2006 (K06), the results show that the SCAPE-M algorithm with an RMSE of 0.002, RE of 17.1% and determination coefficient (R^2) of 0.746 achieved the best performance, followed by the MUMM algorithm (RMSE: 0.004, RE: 18.1%, R^2: 0.646), C2WP (RMSE: 0.005, RE: 33.9%, R^2: 0.590), and GWI (RMSE: 0.010, RE: 70.5%, R^2: 0.444). For the 2008 results (K08), the MUMM algorithm showed the best performance (RMSE: 0.002, RE: 16.9%, R^2: 0.778), followed by SCAPE-M (RMSE: 0.002, RE: 29.9%, R^2: 0.722), C2WP (RMSE: 0.004, RE: 50.5%, R^2: 0.647), and GWI (RMSE: 0.006, RE: 69.9%, R^2: 0.541).

Although the GWI algorithm gave the poorest performance for both the 2006 and 2008 data, it gave the best performance for the 2010 data (K10; RMSE: 0.005, RE: 42.0%, R^2: 0.599). The next-best performances were by MUMM (RMSE: 0.006, RE:

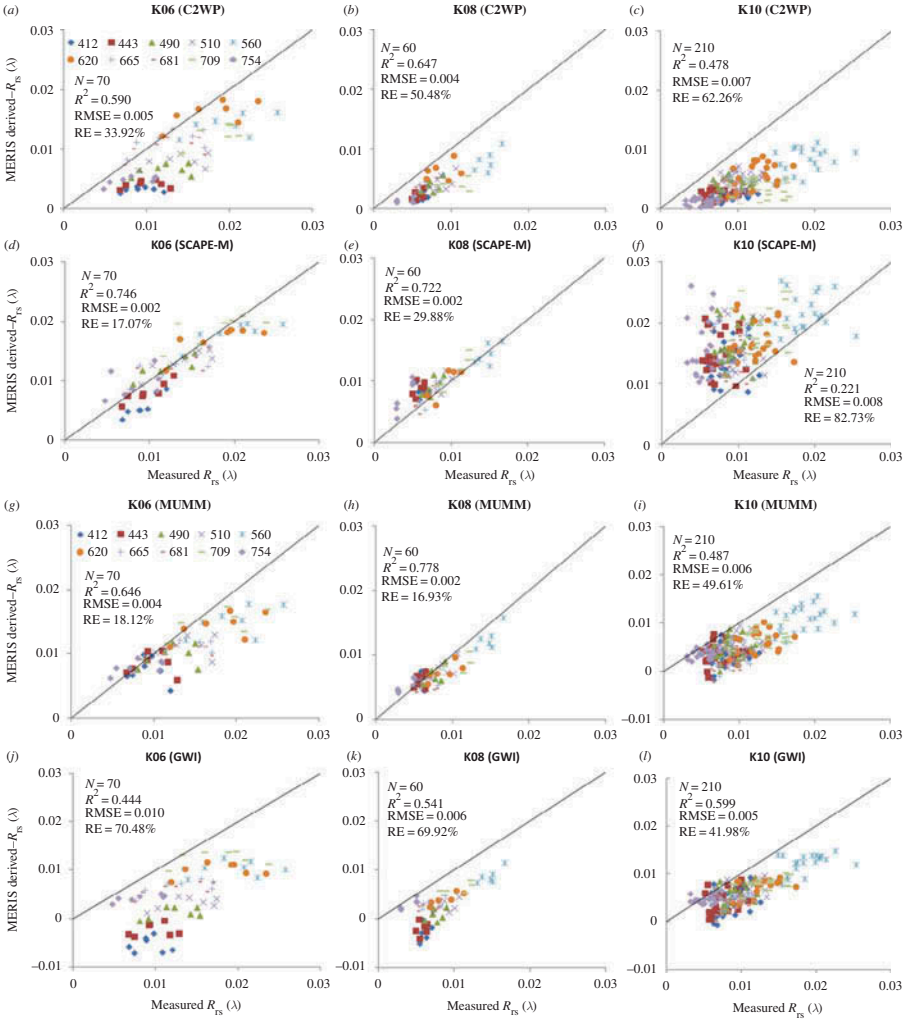

Figure 2. Comparisons between *in situ*-measured and MERIS-derived water-leaving remote-sensing reflectance by the four atmospheric correction algorithms (C2WP, SCAPE-M, MUMM, and GWI) in Lake Kasumigaura, Japan, for MERIS bands 1–10. The centre wavelength at each band is shown in the legend. The black line represents the 1:1 line. Left column, 18 February 2006; middle, 7 August 2008; right, 18 May 2010.

49.6%, R^2: 0.487) and C2WP (RMSE: 0.007, RE: 62.3%, R^2: 0.478). The SCAPE-M algorithm showed the poorest performance for the 2010 data (RMSE: 0.008, RE: 82.7%, R^2: 0.221). It is notable that all four atmospheric correction algorithms showed poorer performance for the 2010 data compared with those of 2006 and 2008.

Figure 3 shows the comparison of RMSE and RE at each MERIS band (1–10) among the four atmospheric correction algorithms for each date. The SCAPE-M algorithm gave the lowest RMSE and RE at most MERIS bands (except for bands 1 and 10 for the 2006 data), whereas the MUMM and GWI algorithms gave the lowest RMSE and RE values at most MERIS bands for the data of 2008 (except for bands 5, 9, and 10) and 2010 (except for band 5), respectively. The C2WP algorithm showed relatively large retrieval errors for

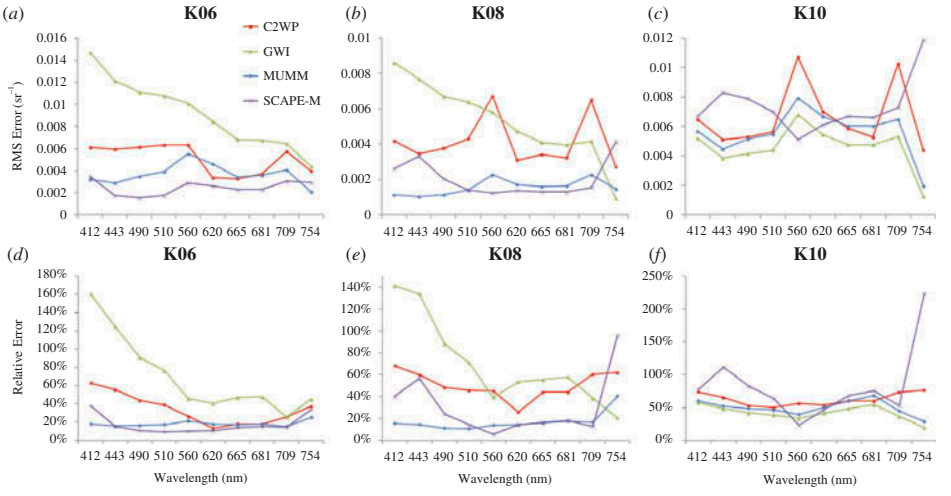

Figure 3. Variation in root mean square error (RMSE, top) and relative error (RE, bottom) as a function of wavelength.

all three dates. In addition, the GWI algorithm showed variations in RMSE and RE as a function of wavelength, while the other three algorithms showed relatively constant RMSE and RE values for all bands, especially for the MUMM algorithm.

3.2. *Performance of the four atmospheric correction algorithms for NIR-red indices*

One of the most important applications of water colour remote sensing is to estimate chlorophyll-*a* concentration, which is a key parameter for assessing water quality, the primary production of phytoplankton, and more. To develop chlorophyll-*a* estimation algorithms, band ratios of water-leaving reflectance are often used (Gitelson 1992; O'Reilly et al. 1998; Gitelson et al. 2008). Here, we selected two band ratio indices for comparison: a two-band index ($R_{rs}(709)/R_{rs}(665)$) and a three-band index ($R_{rs}(753)/R_{rs}(665) - R_{rs}(753)/R_{rs}(709)$), which are widely used in turbid inland waters (Gitelson et al. 2008; Moses et al. 2009). The results are shown in Figures 4 and 5. Generally, the two-band index provided better performance than the three-band index for all four atmospheric correction algorithms. The SCAPE-M algorithm showed good performance (RE 7.84%) for the two-band index for all dates, although it gave a poor performance at each MERIS band for the 2010 data (Figures 2(*d*)–(*f*) and 3). The SCAPE-M algorithm produced overestimation for the three-band index for all dates. The MUMM algorithm showed acceptable performance for the 2006 and 2008 data for both band ratio indices, but poor performance for the 2010 data. The band ratio indices obtained from the GWI and C2WP algorithms showed relatively large errors.

4. Discussion

4.1. *Performance of the C2WP algorithm*

Compared with the other three algorithms, the C2WP algorithm showed lower atmospheric correction accuracies for all three dates, and even for all sampling sites with concentrations of three water constituents within the ranges of the training data (Figures 2

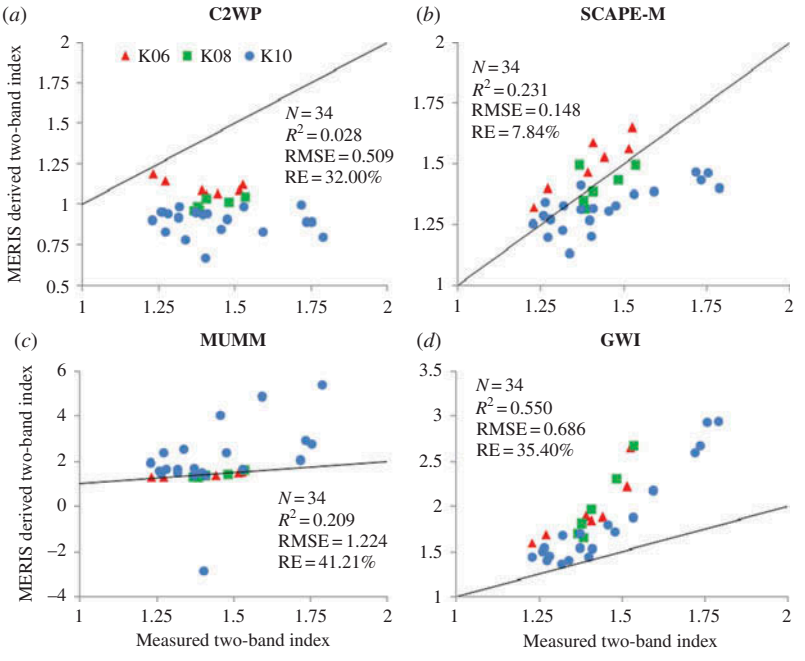

Figure 4. Scatterplots of MERIS-derived vs *in situ*-measured two-band index ($R_{rs}(709)/R_{rs}(665)$) by the algorithms: (*a*) C2WP, (*b*) SCAPE-M, (*c*) MUMM, and (*d*) GWI. The black line represents the 1:1 line.

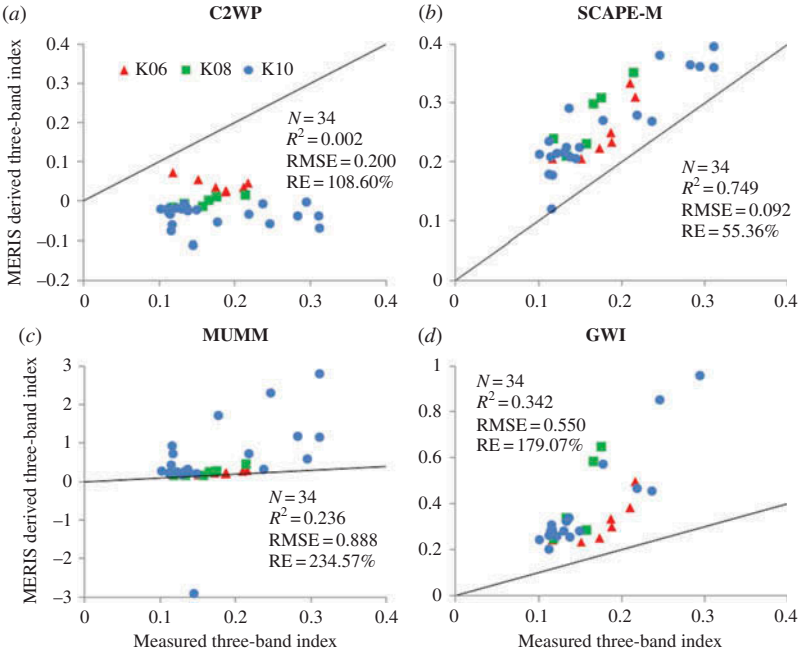

Figure 5. Scatterplots of the MERIS-derived vs *in situ*-measured three-band index ($R_{rs}(753)/R_{rs}(665) - R_{rs}(753)/R_{rs}(709)$) by the algorithms: (*a*) C2WP, (*b*) SCAPE-M, (*c*) MUMM, and (*d*) GWI. The black line represents the 1:1 line.

(*a*)–(*c*) and 3). In addition, by comparing the averaged water-leaving reflectance spectra corrected by C2WP with those corrected by the other three atmospheric correction algorithms as well as *in situ* measurements for each date, we found that the C2WP algorithm changed the spectral shapes after atmospheric correction had been carried out, especially around the reflectance peak at the wavelength of 709 nm (Figure 6; the reflectance peak was smoothed by C2WP). The poor performance of the two-band and three-band indices also indicated that the C2WP algorithm could not reproduce actual

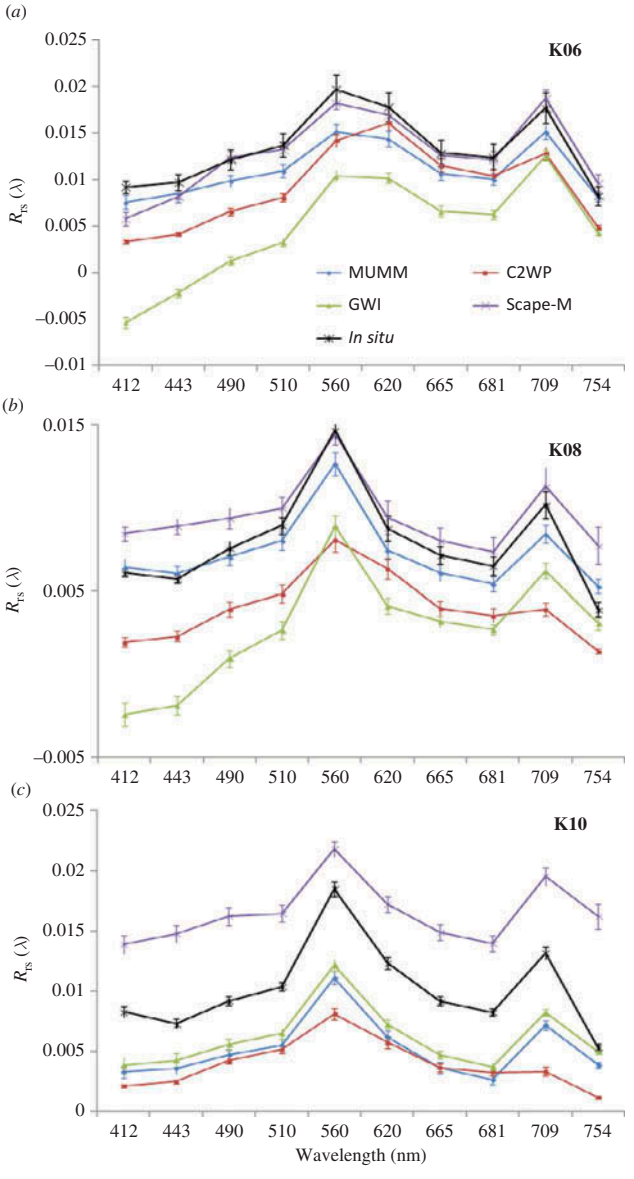

Figure 6. Comparison between *in situ*-measured and averaged MERIS-derived remote-sensing reflectance by the four atmospheric correction algorithms for each date. Error bars refer to the standard deviation calculated from all measurements available for a given date. (*a*) 18 February 2006; (*b*) 7 August 2008; (*c*) 18 May 2010.

spectral shapes well at the wavelength range 665–754 nm (Figures 4(*a*) and 5(*a*)). This is probably because IOPs in Spanish lakes are different from those in Lake Kasumigaura (Yoshimura et al. 2012; Yang et al. 2013). These results strongly suggest that NN parameters should be retrained by a simulation data set on the basis of IOPs collected from target waters.

4.2. *Performance of the SCAPE-M algorithm*

The assumption in the SCAPE-M algorithm for aerosol retrieval is that the atmospheric state should be homogenous within an area of 30 km × 30 km (Guanter, Sanpedro, and Moreno 2007, 2010). Figure 7 shows the average, standard deviation (SD), and coefficients of variation (CV) (CV = SD/average of parameter) of the Rayleigh scattering-corrected remote-sensing reflectance at MERIS band 14 (885 nm) over Lake Kasumigaura. It can be seen that the Rayleigh scattering-corrected remote-sensing reflectance of 2006 (February 18) showed the least spatial variation (SD 0.001), followed by 2008 (August 7, SD 0.005), while that of 2010 (May 18) showed the largest spatial variation (SD 0.012, approximately 12-fold that of 2006 and 2.4-fold that of 2008). In addition, compared with the spatial variation in Rayleigh scattering-corrected remote-sensing reflectance, that of water-leaving reflectance at this band was low for all dates (SD 0.002 for 2006, 0.001 for 2008 and 2010).

These results indicate that the spatial variation in Rayleigh scattering-corrected remote-sensing reflectance at band 14 was mainly caused by the atmospheric status at that time. Therefore, in Figure 7, it is clear that the atmospheric status on 18 May 2010 was the most heterogeneous, followed by 7 August 2008, while that on 18 February 2006 was the most homogeneous. This is the main reason why the SCAPE-M algorithm gave the best performance for the 2006 image, an acceptable atmospheric correction accuracy for the 2008 image, but failed for the 2010 image (Figures 2(*d*)–(*f*)). In addition, visibility at the times of satellite overpass (about 10:00 a.m., local time) was 35 km on 18 February 2006, 15 km on 7 August 2008, and 9 km on 18 May 2010, suggesting that aerosol loadings in the 2006, 2008, and 2010 data were low, moderate, and high, respectively.

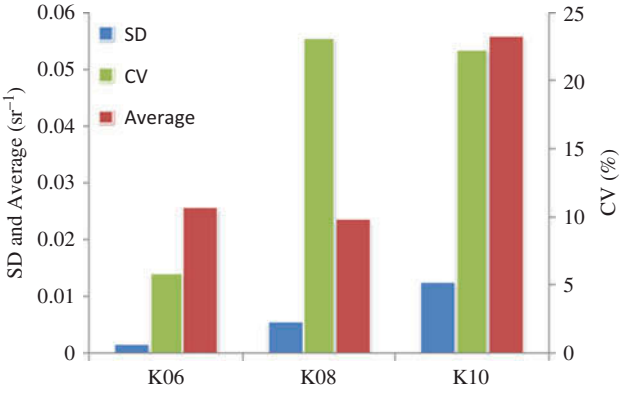

Figure 7. Average, standard deviation (SD), and coefficients of variation (CV) of the Rayleigh scattering-corrected remote-sensing reflectance at MERIS band 14 (885 nm) over Lake Kasumigaura for each date.

It is surprising that the two-band index showed acceptable accuracy even for the 2010 image, when the SCAPE-M algorithm could not yield sufficient accuracy for all single bands (Figures 2(*f*), 3(*c*) and 4(*b*)). The three-band index obtained from SCAPE-M-corrected water-leaving reflectance also showed the best performance among the four atmospheric correction algorithms, even though RE for the four algorithms was low in each case (Figure 5(*b*)). These results indicate that the SCAPE-M algorithm can maintain the actual spectral shape of water-leaving reflectance because it avoided *a priori* assumptions regarding water composition and its spectral response by the use of neighbouring land pixels (Figure 6).

4.3. Performance of the MUMM algorithm

For the successful use of the MUMM algorithm, two assumptions must be valid (Ruddick, Ovidio, and Rijkeboer 2000). The first concerns the atmospheric status over the target waters, which requires that the ratios of multiple-scattering aerosols and aerosol-Rayleigh reflectances at two NIR reference bands are spatially homogeneous over the sub-scene of interest (i.e. they can be assumed to be constant). Although there was a lack of atmospheric data to test this assumption over Lake Kasumigaura, the results shown in Figure 7, suggesting large spatial variation in atmospheric status in the 2010 image, probably make this assumption invalid. This invalid assumption for atmospheric status could be one reason why the MUMM algorithm performed poorly for the 2010 image (Figure 2(*i*)).

The second assumption concerns water composition and its spectral response, which requires that the ratios of water-leaving reflectances normalized by the sun–sea atmospheric transmittance at two NIR reference bands are spatially homogeneous over the sub-scene of interest (i.e. they can be assumed to be constant). *In situ* water-leaving reflectance values were used to test the validity of the second assumption following the method of Doron et al. (2011). Figure 8 shows the relationship between the ratio of $R_{rs}(779)$ and $R_{rs}(865)$ and single $R_{rs}(865)$. $R_{rs}(865)$ has been used as an indicator for water turbidity in previous studies (Ruddick et al. 2006; Doron et al. 2011). Generally, $R_{rs}(865)$ is lower than 10^{-4} for very clear waters, between 10^{-4} and 10^{-2} for moderately turbid to turbid waters, and between 10^{-2} and 10^{-1} for extremely turbid waters (Doron et al. 2011).

From Figure 8, it can be seen that the ratios were not constant as the second assumption required – they decreased with increasing turbidity. This result is similar to that reported by Doron et al. (2011). For MERIS data, the MUMM algorithm uses a constant ratio of 1.711. Compared with this constant value, the average bias of the ratios ($R_{rs}(779)/R_{rs}(865)$) estimated from *in situ* water-leaving reflectance was 8%, 6%, and 13% for 2006, 2008, and 2010, respectively.

Consequently, the performance of the MUMM algorithm for each image can be explained as follows: (1) the moderate performance for the 2006 image occurred because the data for this date met the first assumption (low and homogenous aerosol scattering), but failed for the second assumption (Figure 2(*g*)); (2) the best performance for the 2008 image occurred because the 2008 data met both assumptions relatively well (Figure 2(*h*)); and (3) the poor performance for the 2010 image occurred because both assumptions were not valid for that image (Figure 2(*i*)). These results indicate that limitations of the MUMM algorithm come not only from atmospheric status but also from water constituents and their spectral responses.

4.4. Performance of the GWI algorithm

The assumption in the GWI algorithm is that a bio-optical model can be used to accurately estimate water-leaving reflectance at two NIR reference bands (bands 12 and 13 of the

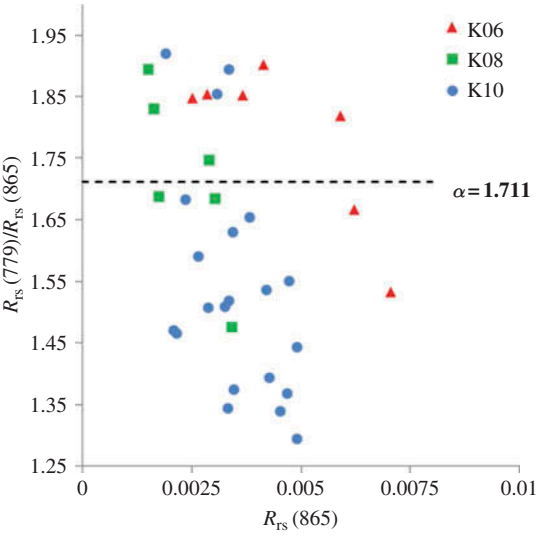

Figure 8. Scatterplots of $R_{rs}(779)/R_{rs}(865)$ vs $R_{rs}(865)$ for *in situ* measurements collected from three field campaigns. The constant value of the ratio $R_{rs}(779)/R_{rs}(865)$ used for MERIS data is 1.711 in SeaDAS, and is depicted as a straight line.

MERIS) through an iterative procedure (Stumpf et al. 2003; Bailey, Franz, and Werdell 2010). Figure 9 shows comparisons between *in situ*-measured and estimated water-leaving reflectance at MERIS bands 12 and 13, respectively. It can be seen that the water-leaving reflectance at the two NIR reference bands were largely underestimated by the bio-optical model, especially for the 2006 and 2008 data (RE 56.0% for band 12, and RE 59.0% for band 13).

These results indicate that the current bio-optical model used in the GWI algorithm is not able to provide sufficient accuracy for estimating water-leaving reflectance at the two NIR reference bands in Lake Kasumigaura. The underestimation of water-leaving reflectance at the two NIR reference bands will result in an overestimation of multiple-scattering aerosols and aerosol-Rayleigh reflectances at these bands, and then an overestimation of aerosol scattering at shorter bands. This is the reason why the atmospherically corrected water-leaving reflectances by the GWI algorithm were underestimated for all dates (Figures 2(*j*)–(*l*)).

4.5. Potential for improving the atmospheric correction algorithm in Lake Kasumigaura

In light of the above analyses, two possibilities can be considered towards improving the existing atmospheric correction algorithms in Lake Kasumigaura for future applications. The first is to improve the C2WP algorithm by retraining the parameters of NN using comprehensive simulation data. It is necessary to obtain the optical properties of water (e.g. IOPs and concentrations of water constituents) and atmosphere (e.g. amount and type of aerosol) in/over Lake Kasumigaura for accurate bio-optical and radiative transfer simulations.

Since Lake Kasumigaura is close to Tokyo, the largest city in Japan (only 60 km away), and several heavy industries are in operation along the Pacific coast, it is often

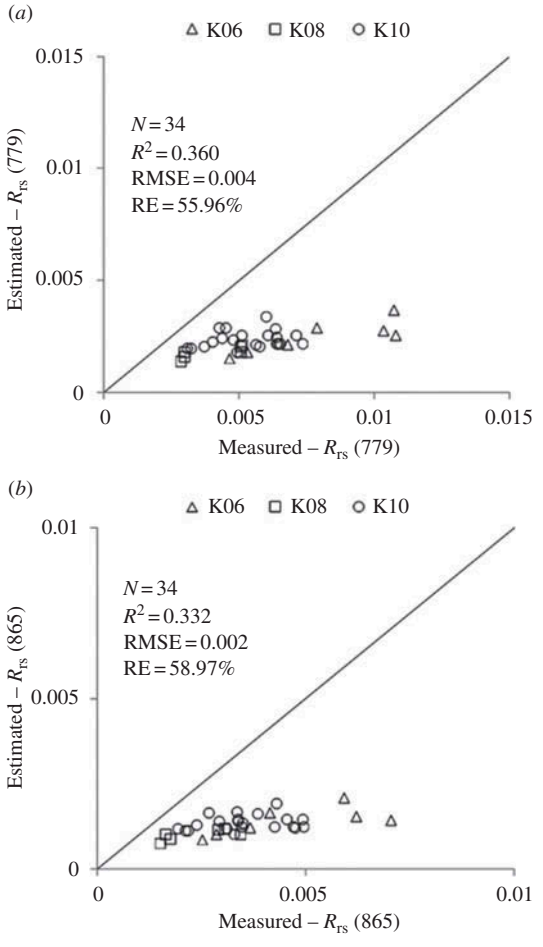

Figure 9. Comparison between *in situ*-measured and estimated water-leaving reflectance at two NIR reference bands. (*a*) MERIS band 12 (779 nm); (*b*) MERIS band 13 (865 nm).

difficult to assume a homogenous atmospheric status (especially for the amount and type of aerosol) over the lake (Figure 7). Therefore, attempts to improve the MUMM and SCAPE-M algorithms for atmospheric correction in Lake Kasumigaura will probably not be successful. This is because both algorithms require the homogenous assumption regarding atmospheric status. Consequently, the second possibility would be to improve the first type of approach (i.e. accurately estimating water-leaving reflectance at two NIR reference wavelengths using a more appropriate method). The bio-optical model used in the GWI algorithm has been shown to be inappropriate for Lake Kasumigaura, mainly because several empirical relationships for estimating absorption and backscattering coefficients were not valid (Figure 9). Extending the reference wavelength from visible to NIR domains can probably provide an opportunity to improve the performance of the bio-optical model (Yang et al. 2013), and thus more accurate atmospheric correction in Lake Kasumigaura. Work in this area is ongoing.

5. Conclusions

Here, we evaluated four atmospheric correction algorithms using *in situ* water-leaving reflectance and concurrently acquired MERIS images collected from Lake Kasumigaura, Japan (turbid inland water). The validity of the assumptions in the four atmospheric correction algorithms was also investigated to understand both the advantages and limitations of each algorithm. The results show that all atmospheric correction algorithms evaluated have limitations in regard to Lake Kasumigaura, although the SCAPE-M and MUMM algorithms had acceptable accuracy for atmospheric correction in several cases (i.e. relative errors less than 30% for the 2006 and 2008 images). The performances of all four algorithms strongly depended on their assumptions (atmospheric status and/or turbidity of water body), and each algorithm failed when its assumptions became invalid (e.g. for the 2010 image, the relative errors ranged from 42% to 83%).

These results indicate that further improvements are necessary to address the issue of atmospheric correction for turbid inland waters such as Lake Kasumigaura. By considering the features of atmosphere and water quality over/in Lake Kasumigaura, the NN technique with more suitable training data and the estimation of water-leaving reflectance at two NIR reference wavelengths using a more appropriate method may improve the existing atmospheric correction algorithms in the lake.

Acknowledgements

The authors would like to acknowledge Dr L. Guanter, who developed the SCAPE-M algorithm and performed atmospheric correction of SCAPE-M on the MERIS images used in this study. The authors would also like to thank the two anonymous referees for their valuable and useful comments on the manuscript.

Funding

This research was supported in part by the Grants-in-Aid for Scientific Research of MEXT from Japan [No. 25420555 and No. 23404015], and also by the Environment Research and Technology Development Fund [S–9–4–(1)] of the Ministry of the Environment, Japan.

References

Aschbacher, J., and M. P. M. Pérez. 2012. "The European Earth Monitoring (GMES) Programme: Status and Perspectives." *Remote Sensing of Environment* 120: 3–8. doi:10.1016/j.rse.2011.08.028.

Ayres, W. S., A. Busia, A. Dinar, R. Hirji, S. F. Lintner, A. F. McCalla, and R. Robelus. 1996. *Integrated Lake and Reservoir Management: World Bank Approach and Experience*. Washington, DC: World Bank.

Bailey, S. W., B. A. Franz, and P. J. Werdell. 2010. "Estimation of Near-Infrared Water-Leaving Reflectance for Satellite Ocean Color Data Processing." *Optics Express* 18: 7521–7527. doi:10.1364/OE.18.007521.

CGER. 2010. Lake Kasumigaura Database. National Institute for Environmental Studies, Japan. Accessed August 1, 2012. http://db.cger.nies.go.jp/gem/moni-e/inter/GEMS/database/kasumi/index.html.

Doerffer, R., and H. Schiller. 2007. "The MERIS Case 2 Water Algorithm." *International Journal of Remote Sensing* 28: 517–535. doi:10.1080/01431160600821127.

Doerffer, R., and H. Schiller. 2008. *MERIS Regional Coastal and Lake Case 2 Water Project – Atmospheric Correction ATBD*, GKSS Research Center 21502, Version 1.0, Geesthacht.

Doron, M., S. Bélanger, D. Doxaran, and M. Babin. 2011. "Spectral Variations in the Near-Infrared Ocean Reflectance." *Remote Sensing of Environment* 115: 1617–1631. doi:10.1016/j.rse.2011.01.015.

Duan, H., R. Ma, S. G. H. Simis, and Y. Zhang. 2012. "Validation of MERIS Case-2 Water Products in Lake Taihu, China." *GIScience & Remote Sensing* 49: 873–894. doi:10.2747/1548–1603.49.6.873.

Fukushima, T., J. Park, A. Imai, and K. Matsushige. 1996. "Dissolved Organic Carbon in a Eutrophic Lake; Dynamics, Biodegradability and Origin." *Aquatic Sciences* 58: 139–157. doi:10.1007/BF00877112.

Giardino, C., M. Pepe, P. A. Brivio, P. Ghezzi, and E. Zilioli. 2001. "Detecting Chlorophyll, Secchi Disk Depth and Surface Temperature in a Sub-Alpine Lake Using Landsat Imagery." *Science of the Total Environment* 268: 19–29. doi:10.1016/S0048–9697(00)00692–6.

Gitelson, A. A. 1992. "The Peak Near 700 Nm on Reflectance Spectra of Algae and Water: Relationships of Its Magnitude and Position with Chl. Concentration." *International Journal of Remote Sensing* 13: 3367–3373.

Gitelson, A. A., G. Dall'Olmo, W. J. Moses, D. C. Rundquist, T. Barrow, T. R. Fisher, D. Gurlin, and J. Holz. 2008. "A Simple Semi-Analytical Model for Remote Estimation of Chlorophyll-a in Turbid Waters: Validation." *Remote Sensing of Environment* 112: 3582–3593. doi:10.1016/j.rse.2008.04.015.

Gordon, H. R., and M. Wang. 1994. "Retrieval of Water-Leaving Radiance and Aerosol Optical Thickness over the Oceans with SeaWiFS: A Preliminary Algorithm." *Applied Optics* 33: 443–452. doi:10.1364/AO.33.000443.

Guanter, L., M. Del Carmen González-Sanpedro, and J. Moreno. 2007. "A Method for the Atmospheric Correction of ENVISAT/MERIS Data Over Land Targets." *International Journal of Remote Sensing* 28: 709–728. doi:10.1080/01431160600815525.

Guanter, L., A. Ruiz-Verdú, D. Odermatt, C. Giardino, S. Simis, V. Estellés, T. Heege, J. A. Dominguez-Gómez, and J. Moreno. 2010. "Atmospheric Correction of ENVISAT/MERIS Data over Inland Waters: Validation for European Lakes." *Remote Sensing of Environment* 114: 467–480. doi:10.1016/j.rse.2009.10.004.

Han, L., and K. J. Jordan. 2005. "Estimating and Mapping Chlorophyll-a Concentration in Pensacola Bay, Florida, Using Landsat ETM+ Data." *International Journal of Remote Sensing* 26: 5245–5254. doi:10.1080/01431160500219182.

Hu, C., K. L. Carder, and F. E. Muller-karger. 2000. "Atmospheric Correction of SeaWiFS Imagery Over Turbid Coastal Waters: A Practical Method." *Remote Sensing of Environment* 74: 195–206. doi:10.1016/S0034–4257(00)00080–8.

IOCCG. 2010. *Reports of the International Ocean-Colour Coordinating Group No. 10: Atmospheric Correction for Remotely-Sensed Ocean-Colour Products, edited by Wang, Menghua.* Dartmouth: IOCCG.

Jamet, C., H. Loisel, C. P. Kuchinke, K. G. Ruddick, G. Zibordi, and H. Feng. 2011. "Comparison of Three SeaWiFS Atmospheric Correction Algorithms for Turbid Waters Using AERONET-OC Measurements." *Remote Sensing of Environment* 115: 1955–1965. doi:10.1016/j.rse.2011.03.018.

Kuchinke, C. P., H. R. Gordon, and B. A. Franz. 2009. "Spectral Optimization for Constituent Retrieval in Case 2 Waters I: Implementation and Performance." *Remote Sensing of Environment* 113: 571–587. doi:10.1016/j.rse.2008.11.001.

Kuchinke, C. P., H. R. Gordon, L. W. Harding Jr, and K. J. Voss. 2009. "Spectral Optimization for Constituent Retrieval in Case 2 Waters II: Validation Study in the Chesapeake Bay." *Remote Sensing of Environment* 113: 610–621. doi:10.1016/j.rse.2008.11.002.

Liu, Y., Md. A. Islam, and J. Gao. 2003. "Quantification of Shallow Water Quality Parameters by Means of Remote Sensing." *Progress in Physical Geography* 27: 24–43. doi:10.1191/0309133303pp357ra.

Mobley, C. D. 1999. "Estimation of the Remote-Sensing Reflectance from Above-Surface Measurements." *Applied Optics* 38: 7442–7455. doi:10.1364/AO.38.007442.

Moses, W. J., A. A. Gitelson, S. Berdnikov, and V. Povazhnyy. 2009. "Estimation of Chlorophyll-a Concentration in Case II Waters Using MODIS and MERIS Data–Successes and Challenges." *Environmental Research Letters* 4: 045005. doi:10.1088/1748–9326/4/4/045005.

O'Reilly, J. E., S. Maritorena, B. G. Mitchell, D. A. Siegel, K. L. Carder, S. A. Garver, M. Kahru, and C. McClain. 1998. "Ocean-Color Chlorophyll Algorithms for SeaWiFS." *Journal of Geophysical Research* 103 (C11): 24937–24953. doi:10.1029/98JC02160.

Oyama, Y., B. Matsushita, T. Fukushima, K. Matsushige, and A. Imai. 2009. "Application of Spectral Decomposition Algorithm for Mapping Water Quality in a Turbid Lake (Lake

Kasumigaura, Japan) from Landsat TM Data." *ISPRS Journal of Photogrammetry and Remote Sensing* 64: 73–85. doi:10.1016/j.isprsjprs.2008.04.005.

Ramon, D., and R. Santer. 2005. "Aerosol over Land with MERIS, Present and Future." In Proceedings of the MERIS and AATSR Workshop 2005, ESA SP-597, ESRIN, Frascati, September 26–30.

Ruddick, K. G., V. De. Cauwer, Y.-Je. Park, and G. Moore. 2006. "Seaborne Measurements of Near Infrared Water-Leaving Reflectance: The Similarity Spectrum for Turbid Waters." *Limnology and Oceanography* 51: 1167–1179. doi:10.4319/lo.2006.51.2.1167.

Ruddick, K. G., F. Ovidio, and M. Rijkeboer. 2000. "Atmospheric Correction of SeaWiFS Imagery for Turbid Coastal and Inland Waters." *Applied Optics* 39: 897–912. doi:10.1364/AO.39.000897

Santer, R., J. Vidot, and O. Aznay. 2005. "Standard Aerosol Model Families Used for Atmospheric Correction: How Comparable Are They? How Valid Are They?" In Proceedings of the MERIS and AATSRWorkshop 2005, ESA SP-597, ESRIN, Frascati, September 26–30.

Schroeder, T. H., I. Behnert, M. Schaale, J. Fischer, and R. Doerffer. 2007. "Atmospheric Correction Algorithm for MERIS Above Case-2 Waters." *International Journal of Remote Sensing* 28: 1469–1486. doi:10.1080/01431160600962574.

Schroeder, T. H., M. Schaale, and J. Fischer. 2007. "Retrieval of Atmospheric and Oceanic Properties from MERIS Measurements: A New Case-2 Water Processor for BEAM." *International Journal of Remote Sensing* 28: 5627–5632. doi:10.1080/01431160701601774.

SCOR-UNESCO. 1966. "Determination of Photosynthetic Pigment in Seawater." In *Monographs on Oceanographic Methodology,* Vol. 1., 11–18. Paris: SCOR-UNESCO.

Shi, W., and M. Wang. 2007. "Detection of Turbid Waters and Absorbing Aerosols for the MODIS Ocean Color Data Processing." *Remote Sensing of Environment* 110: 149–161. doi:10.1016/j.rse.2007.02.013.

Shi, W., and M. Wang. 2009. "An Assessment of the Black Ocean Pixel Assumption for MODIS SWIR Bands." *Remote Sensing of Environment* 113: 1587–1597. doi:10.1016/j.rse.2009.03.011.

Stumpf, R. P., R. A. Arnone, R. W. Gould, P. M. Martinolich, and V. Ransibrahmanakul. 2003. "A Partly Coupled Ocean-Atmosphere Model for Retrieval of Water-Leaving Radiance From SeaWiFS in Coastal Waters." In *SeaWiFS Postlaunch Technical Report Series, NASA Technical Memorandum 2003–206892,* Vol. 22, edited by S. B. Hooker and E. R. Firestone, 51–59. Greenbelt, MD: NASA Goddard Space Flight Center.

Wang, M., and W. Shi. 2007. "The NIR-SWIR Combined Atmospheric Correction Approach for MODIS Ocean Color Data Processing." *Optics Express* 15: 15722. doi:10.1364/OE.15.015722.

Wang, M., W. Shi, and L. Jiang. 2012. "Atmospheric Correction Using Near-Infrared Bands for Satellite Ocean Color Data Processing in the Turbid Western Pacific Region." *Optics Express* 20: 741–753. doi:10.1364/OE.20.000741.

Wang, M., W. Shi, and J. Tang. 2011. "Water Property Monitoring and Assessment for China's Inland Lake Taihu from MODIS-Aqua Measurements." *Remote Sensing of Environment* 115: 841–854. doi:10.1016/j.rse.2010.11.012.

Wang, M., S. Son, and W. Shi. 2009. "Evaluation of MODIS SWIR and NIR-SWIR Atmospheric Correction Algorithms Using SeaBASS Data." *Remote Sensing of Environment* 113: 635–644. doi:10.1016/j.rse.2008.11.005.

Yang, W., B. Matsushita, J. Chen, K. Yoshimura, and T. Fukushima. 2013. "Retrieval of Inherent Optical Properties for Turbid Inland Waters from Remote-Sensing Reflectance." *IEEE Transactions on Geoscience and Remote Sensing* 51: 3761–3773. doi:10.1109/TGRS.2012.2220147.

Yoshimura, K., N. Zaitsu, Y. Sekimura, B. Matsushita, T. Fukushima, and A. Imai. 2012. "Parameterization of Chlorophyll A-Specific Absorption Coefficients and Effects of Their Variations in a Highly Eutrophic Lake: A Case Study at Lake Kasumigaura, Japan." *Hydrobiologia* 691: 157–169. doi:10.1007/s10750-012-1066-4.